ChemComm

Accepted Manuscript

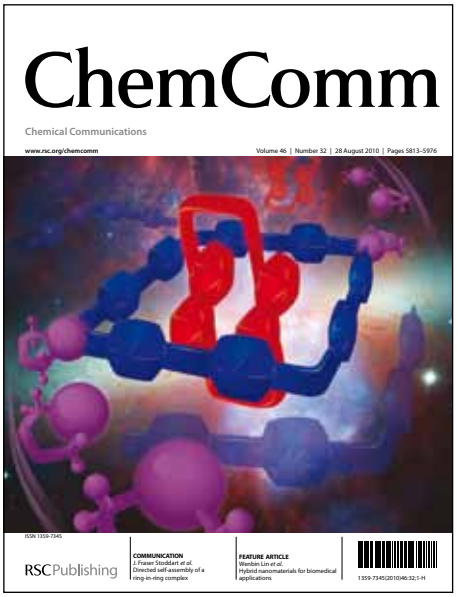

This is an *Accepted Manuscript*, which has been through the RSC Publishing peer review process and has been accepted for publication.

Accepted Manuscripts are published online shortly after acceptance, which is prior to technical editing, formatting and proof reading. This free service from RSC Publishing allows authors to make their results available to the community, in citable form, before publication of the edited article. This *Accepted Manuscript* will be replaced by the edited and formatted *Advance Article* as soon as this is available.

To cite this manuscript please use its permanent Digital Object Identifier (DOI®), which is identical for all formats of publication.

More information about *Accepted Manuscripts* can be found in the **Information for Authors**.

Please note that technical editing may introduce minor changes to the text and/or graphics contained in the manuscript submitted by the author(s) which may alter content, and that the standard **Terms & Conditions** and the **ethical guidelines** that apply to the journal are still applicable. In no event shall the RSC be held responsible for any errors or omissions in these *Accepted Manuscript* manuscripts or any consequences arising from the use of any information contained in them.

Chem. Commun.

RSCPublishing

COMMUNICATION

Unprecedented redox-driven ligand ejection in nickel(II)-diiminosemiquinonate radical complexes

Cite this: DOI: 10.1039/x0xx00000x

N. Leconte,* J. Ciccione, G. Gellon, C. Philouze and F. Thomas*

Received 00th January 2012,
Accepted 00th January 2012

DOI: 10.1039/x0xx00000x

www.rsc.org/

Nickel(II) complexes of (M:L) stoichiometries 1:1 (1) and 1:2 (2) were prepared from a polydentate ligand involving diiminosemiquinonate radicals. Both were characterized by X-ray diffraction, Vis-NIR and EPR spectroscopy as well as electrochemistry. Ligand-centered oxidation of 1 promotes ligand ejection to give 2.

Molecular switches are at the heart of molecular electronic devices and find applications in numerous fields like biosensors,[1] drug delivery,[2] nanotechnologies... [3] They refer to molecular systems capable of undergoing reversible chemical and physical changes triggered by external stimuli such as electric current, light or pH. [4] Among the platforms developed for this purpose inorganic complexes play a central role. Redox events on the metal can indeed trigger changes in its geometrical preference, and induce subsequent reorganization of the surrounding ligands. [5] Inorganic molecular switches that function with ligand-based redox events are rarer, [6] although organic molecular switches have been widely developed during the past decade. [4] Protypical organic moieties that respond to a redox stimulus by molecular motion are viologen pairs. [7] The viologens do indeed not interact one with each other under their cationic forms, but they readily assemble into donor-acceptor pairs (π-dimers) when one of them is reduced. [7]

An alternative, yet less common, approach consists in exploiting the redox activity of one chelating moiety of the ligand to labilize a M-L bond (organic-based redox hemilabile ligands, oRHLs) and induce structural changes. [6] Unfortunately, in these cases rearrangements are often limited to subtle modifications of the metal coordination sphere (Scheme 1a-c), making molecular motions rather small. [8-10]

We herein describe two nickel(II) complexes **1** and **2** prepared from a polydentate *o*-phenylenediamine ligand H_4L (Fig. 1) and show that **2** is capable of large redox-triggered molecular rearrangements. The process, under the form of a reversible ligand ejection affording **1**, is initiated by electron-transfer from the one-electron oxidized *o*-phenylenediamine group.

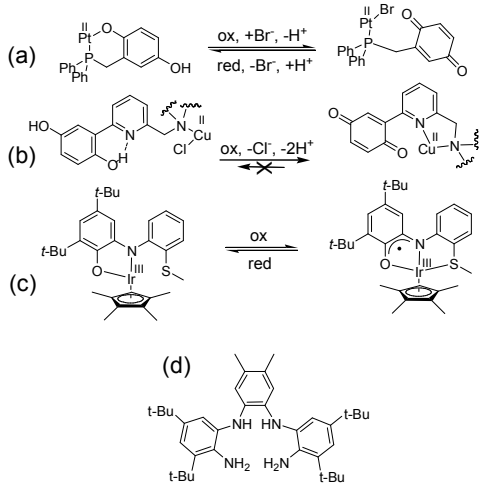

Scheme 1 Redox-switchable ligands involving phenols [(a),[8] (b) [9] and (c) [10]] and molecular formula of H_4L (d).

H_4L (Scheme 1) was synthesized in a two-step sequence from 3,5-di-*tert*-butyl-2-nitrobromobenzene and 4,5-dimethyl-*o*-phenylenediamine (see ESI for details). H_4L reacted with an equimolar amount $Ni(OAc)_2 .4 H_2O$ in the presence of Et_3N to give a brown solution, from which complex **1** precipitated out as a dark solid after exposure to air (yield 76 %). Single crystals of **1** suitable for X-Ray diffraction were grown by slow evaporation of an Et_2O/MeOH solution.

The structure of **1** (Fig. 1a) shows a square planar nickel(II) ion coordinated to a dianionic tetradentate ligand. The Ni-N1, Ni-N2, Ni-N3 and Ni-N4 bond distances (1.809(3), 1.807(2), 1.816(3) and 1.807(3) Å, respectively) are consistent with a diamagnetic low-spin configuration of the metal ion. The peripherical C1-N1, C7-N4 bond lengths (1.343(4) and 1.344(4) Å respectively) and C2-N2, C8-N3 bond lengths (1.366(4) and 1.364(4) Å, respectively) are significantly shorter than the central C13-N2 and C14-N3 ones (1.423(4) and 1.416(4) Å, respectively), but longer than those

expected for C=N bonds. The central ring has thus a dianionic diamidobenzene character, whereas the peripherical rings are diiminobenzosemiquinone (ISQ) radicals. [11] Noteworthy, the three aromatic rings are coplanar: a strong antiferromagnetic coupling is thus expected between the two radical spins, leading to the observed diamagnetism.

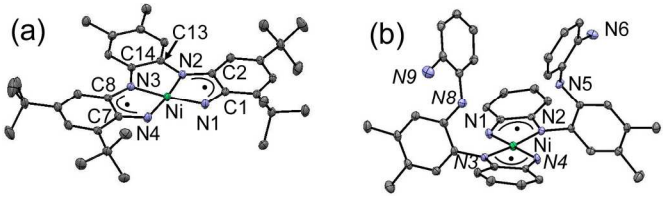

Figure 1 X-Ray crystal structures of: (a) [NiL] **(1)** and (b) [Ni(H$_2$L)$_2$] **(2)** shown with 30% thermal ellipsoids. H atoms (**1** and **2**) and *t*-Bu groups (**2**) are omitted for clarity.

During the synthesis of **1** we made the intriguing observation that a green solution formed instead of the brownish one in ten-times more concentrated media. A simple filtration allowed us to isolate a green solid **2** (yield 66 %), whose formulation clearly differs from that of **1** (Fig. 1b). Although we systematically worked with a (1:1) ligand:metal ratio **2** is constituted by a single metal coordinated to two ligands coordinated in a bidentate fashion. The nickel(II) ion lies in a square planar geometry, while the C1-N1, C7-N4, C2-N2 and C8-N3 bond distances (1.343(3), 1.311(3), 1.359(3) and 1.362(3) Å, respectively) compare fairly with those obtained for **1**, confirming that **2** also contains a bis{ISQ} core. The non-coordinating rings exhibit typical diaminobenzene metrical parameters. It is worth noting that H-bonds exist between N2 and H5 (and opposite N3 and H8), as evidenced by the N2-H5-N5 and N3-H8-N8 bond angles of 110(3)° and 113(3)°, respectively, as well as the bond distances N2-N5 and N3-N8 of 2.780(3) and 2.782(3) Å, respectively.

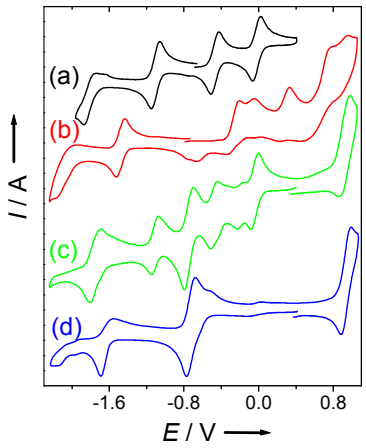

Figure 2. Cyclic voltammetry curves of (a): **1**; (b): **2**; (c): **2** after electrolysis at 0.21 V; (d): H$_4$L after electrolysis at 0.21 V. Concentrations are 0.5 mM (**1**) and 0.25mM (**2**) in CH_2Cl_2 solutions (+ 0.1 M TBAP). *T* = 298 K, scan rate = 0.1 V /s. The potentials are given vs. the Fc^+/Fc reference.

The electrochemical behaviour of **1** and **2** has been investigated by cyclic voltammetry (CV) (Fig. 2). **1** undergoes four reversible monoelectronic transfers (Fig. 2a); two in oxidation at $E_{1/2}^{ox,1}$ = -0.40 V, $E_{1/2}^{ox,2}$ = 0.02 V and two in reduction at $E_{1/2}^{red,1}$ = -0.93 V, $E_p^{c,2}$ = -1.57 V vs. Fc^+/Fc. The oxidation processes are assigned to the successive oxidation of the ISQ moieties [12] into diiminobenzoquinone (IBQ) (Scheme 2).

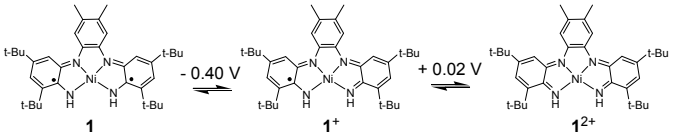

Scheme 2. Sequential oxidation of **1**.

The CV curve of **2** contrast sharply with that of **1**: Oxidation waves were indeed observed at $E_p^{a,1}$ = -0.18, $E_p^{a,2}$ = -0.04 V, $E_p^{a,3}$ = 0.28 V (Fig. 2b), but they were found to be surprisingly irreversible. This prompted us to investigate the electrochemical behaviour of the free ligand H$_4$L (see ESI). H$_4$L also showed irreversible oxidation waves in this potential range ($E_p^{a,1}$ = 0.02, $E_p^{a,2}$ = 0.13 V, $E_p^{a,3}$ = 0.36 V), supporting the assignment of the first anodic waves of **2** to the oxidation of the uncoordinated diaminobenzene moieties. The anodic shift of the coordinated-IBQ/ISQ redox wave when **2** is compared to **1**, most likely results from the presence of H-bonds between N2 and H5 as well as N3 and H8.

After exhaustive electrolysis at +0.21 V the CV curve of **2** was dramatically different than the original one (Fig 2c); it displays a single reversible bielectronic oxidation wave at $E_{1/2}^{ox,1}$ = 0.78 V, and five reversible reduction wave at $E_{1/2}^{red,1}$ = -0.03 V, $E_{1/2}^{red,2}$ = -0.40 V, $E_{1/2}^{red,3}$ = -0.62 V, $E_{1/2}^{red,4}$ = -0.93 V and $E_{1/2}^{red,5}$ = -1.47 V. $E_{1/2}^{red,3}$ corresponds to a bielectronic process, whereas the other reduction waves are monoelectronic processes. The four monoelectronic redox waves are reminiscent of **1** (or its oxidation products). Owing to the electrolysis potential (+0.21 V), which is higher than $E_{1/2}^{ox,2}$ of **1**, the oxidation product is the cation $\mathbf{1}^{2+}$, a fact confirmed by Vis-NIR spectroscopy. Generation of $\mathbf{1}^{2+}$ implies that free ligand is released in solution. A pure sample of H$_4$L was thus subjected to electrolysis under similar conditions. The CV curve recorded after electrolysis shows two reversible two-electron redox waves at $E_{1/2}^{ox,1}$ = 0.79 V and $E_{1/2}^{red,3}$ = -0.61 V (Fig. 2d). Both match the bielectronic waves observed for **2** after oxidation at +0.21 V, confirming that oxidation of **2** is accompanied by release of free oxidized ligand (Scheme 3).

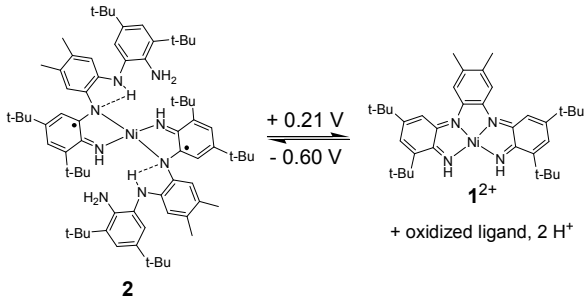

Scheme 3. Redox-driven structural changes in **2**.

We additionally examined the oxidation processes by spectroelectrochemistry (Fig. 3-4). The electronic spectrum of **1** is characterized by an intense LLCT transition involving the ISQ radical at 952 nm [12 050 M^{-1} cm^{-1}], which shifts to 899 nm [11 320 M^{-1} cm^{-1}] in $\mathbf{1}^+$.[13] Not surprisingly the dication $\mathbf{1}^{2+}$ does not exhibit strong ISQ radical band above 850 nm, but simply CT transitions involving the IBQ moieties at 738 nm [7510 M^{-1} cm^{-1}] and 466 nm

[26380 M^{-1} cm^{-1}]. Interestingly the LLCT transition in **2** is four-times more intense than for **1** [877 nm, 55 160 M^{-1} cm^{-1}]. This enhancement may reflect the involvement of the coordinated diaminobenzene bridge in the transition for **1**. During electrolysis of **2** the 877 nm band disappeared at the expense of two intense transitions at 410 [26 100 M^{-1} cm^{-1}] and 494 nm [22 600 M^{-1} cm^{-1}], and a broad band at ca. 700 nm (Fig. 4b). The latter two bands correspond to $\mathbf{1}^{2+}$ (Fig. 3c), whereas the former originates from the oxidized free ligand (see ESI). These spectroscopic results again support a redox-driven ligand ejection, consistent with electrochemical data.

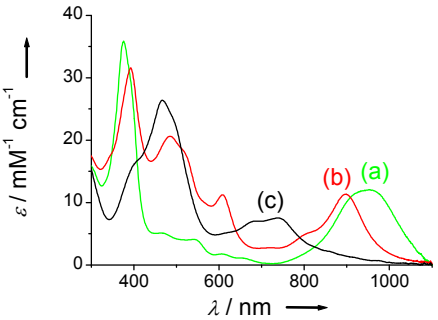

Figure 3. Vis-NIR spectra of (a) **1**, (b) $\mathbf{1}^{+}$, (c) $\mathbf{1}^{2+}$. Concentrations = 0.5 mM in CH_2Cl_2 (+ 0.1 M TBAP). *T* = 298 K.

We monitored the reversibility of the system by applying to **2** the required potential to eject one ligand (exhaustive electrolysis at +0.21 V), and then a cathodic potential (-0.60 V). The Vis-NIR spectrum recorded just after electrolysis (Fig. 4c) was clearly different than that of **2**, with a maximum peak at 894 nm [18 460 M^{-1} cm^{-1}] and a shoulder at 950 nm. However, after 15 h the NIR band has both shifted to 877 nm and increased in intensity (Fig. 4d), giving spectral features reminiscent of **2**. Thus, although the reaction occurs slowly the ejected ligand can rebind the nickel ion after reduction (Scheme 3). [14]

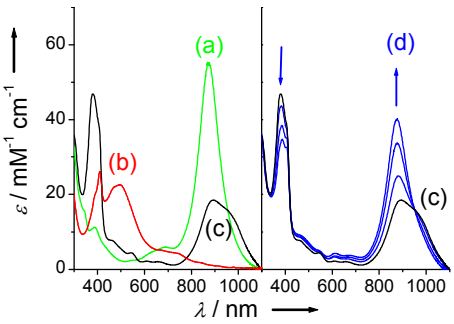

Figure 4. Vis-NIR spectra of (a): **2**; (b): **2** after electrolysis at 0.21 V; (c-d): **2** after electrolysis at 0.21 V followed by reduction at -0.60 V [(c) 5 min after reduction, (d) after 30 min, 2 h and 15 h]. Arrows indicate spectral changes. Concentrations = 0.25 mM in CH_2Cl_2 (+ 0.1 M TBAP). *T* = 298 K.

In conclusion we herein describe the first example of electrochemically driven ejection of a redox hemilabile ligand involving diiminosemiquinonate moieties. Both the intramolecular H-bonds and the attenuated negative charge at the terminal chelating atoms in **2** labilize sufficiently the M-diiminosemiquinonate bonds to allow for redox-triggered ligand ejection, while keeping rebinding possible. The effect of the pH and substituents on the process are currently investigated in our laboratory.

This research has been funded by a grant from the University Joseph Fourier (fond d'intervention) and the Labex ARCANE.

Notes and references

Département de Chimie Moléculaire - Chimie Inorganique Redox (CIRE) - UMR CNRS 5250, Université Joseph Fourier, B. P. 53, 38041 Grenoble cedex 9, France.
Email : fabrice.thomas@ujf-grenoble.fr

† Electronic Supplementary Information (ESI) available: CCDC-927235-6, experimental procedures, EPR, NMR, UV-Vis spectra and cyclic voltammetry curves. See DOI: 10.1039/c000000x/

1 J. W. Canary, S. Mortezaei, J. Liang, *Coord. Chem. Rev.* 2010, **254**, 2249; K. W. Plaxco, H. T. Soh, *Trends. Biotechnol.* 2011, **29**, 1.
2 Y. L. Zhao, Z. Li, S. Kabehie, Y. Y. Botros, J. F. Stoddart, J. I. Zink, *J. Am. Chem. Soc.* 2010, **132**, 13016.
3 B. Y. Ahn, E. B. Duoss, M. J. Motala, X. Guo, S. I. Park, Y. Xiong, J. Yoon, R. G. Nuzzo, J. A. Rogers, J. A. Lewis, *Science* 2009, **232**, 1590.
4 B. L. Feringa, Molecular Switches. Wiley-VCH: Weinheim, Germany, 2001.
5 S. Zahn, J. W. Canary, *Science* 2000, **288**, 1404; B. Champin, P. Mobian, J.-P. Sauvage, *Chem. Soc. Rev.* 2007, **36**, 358. G. Periyasamy, J. P. Collin, J.-P. Sauvage, F. Remacle, *Chem. Eur. J.* 2009, **15**, 1310.
6 A. M. Allgeirer, C. A. Mirkin, *Angew. Chem. Int. Ed.* 1998, **37**, 894.
7 For recent articles see: H. Li, A. C. Fahrenbach, A. Coskun, Z. Zhu, G. Barin, Y. L. Zhao, Y. Y. Botros, J. P. Sauvage, J. F. Stoddart, *Angew. Chem. Int. Ed.* 2011, **50**, 6782. A. Iordache, M. Oltean, A. Milet, F. Thomas, B. Baptiste, E. Saint-Aman, C. Bucher, *J. Am. Chem. Soc.* 2012, **134**, 2653; G. Barin, M. Frasconi, S. M. Dyar, J. Iehl, O. Buyukcakir, A. A. Sarjeant, R. Carmieli, A. Coskun, M. R. Wasielewski, J. F. Stoddart, *J. Am. Chem. Soc.* 2013, **135**, 2466.
8 S. M. Sembiring, S. B. Collbran, D. C. Craig, *Inorg. Chem.* 1995, **34**, 761.
9 Z. He, S. B. Colbran, D. C. Craig, *Chem. Eur. J.* 2003, **9**, 116.
10 R. Hubner, S. Weber, S. Strobel, B. Sarkar, S. Zalis, W. Kaim, *Organometallics* 2011, **30**, 1414.
11 D. Herebian, E. Bothe, F. Neese, T. Weyhermüller, K. Wieghardt, *J. Am. Chem. Soc.* 2003, **125**, 9116.
12 The electrochemically generated $\mathbf{1}^{+}$ is paramagnetic (S = 1/2). It exhibits a slightly rhombic EPR signal at g_1 = 1.994, g_2 = 2.004, g_3 = 2.021. These values are consistent with a main ligand radical character of the singly occupied MO (M. Orio, O. Jarjayes, H. Kanso, C. Philouze, F. Neese, F. Thomas, *Angew. Chem. Int. Ed.* 2010, **49**, 4989).
13 The NIR band of **1** and **2** is assigned to an IVCT transition involving the peripherical ISQ moieties; It formally corresponds to the transfer of an electron from one ISQ group to the other one, and could be formulated as $(ISQ)Ni^{II}(ISQ)\rightarrow(phenylenediamine)Ni^{II}(IBQ)$; The NIR band of $\mathbf{1}^{+}$ reflects the mixed-valent character of this compound. It is ascribed to the $(ISQ)Ni^{II}(IBQ)\rightarrow(IBQ)Ni^{II}(ISQ)$ transition. See ref. 11.
14 The potential of -0.60 V is not sufficient to reduce the oxidized free ligand. The driving force for the conversion $\mathbf{1}^{2+}\rightarrow$ **2** is therefore not electron transfer to the free ligand, but rather to the complex. This

assumption is confirmed by the conversion of **1** into **2** upon addition of H_4L (see ESI).

